Individual differences in time-varying and stationary brain connectivity during movie watching from childhood to early adulthood: Effects of age, sex, and behavioral associations

Xin Di[1*], Ting Xu[2], Lucina Q. Uddin[3], Bharat B. Biswal[1*]

1. Department of Biomedical Engineering, New Jersey Institute of Technology, Newark, NJ 07102, USA

2. Center for the Developing Brain, Child Mind Institute, New York, NY 10022, USA

3. Department of Psychiatry and Biobehavioral Sciences, University of California at Los Angeles, Los Angeles, CA 90095, USA

* Corresponding author:

Xin Di, Ph.D.

604 Fenster Hall, University Height

Newark, NJ, 07102, USA

xin.di@njit.edu

Bharat B. Biswal, Ph.D.

607 Fenster Hall, University Height

Newark, NJ, 07102, USA

bbiswal@yahoo.com

Running title: Individual differences in connectivity

Abstract

Spatially remote brain regions show dynamic functional interactions during various task conditions. Time-varying functional connectivity measured during movie watching was sensitive to movie content, while stationary functional connectivity remains stable across videos. Therefore, it has been suggested that dynamic and stationary functional interactions may reflect different aspects of brain function. However, how individual differences in time-varying and stationary connectivity are associated with behavioral phenotypes is still unclear. We analyzed an open-access functional MRI dataset collected from participants (5 to 22 years old) as they watched two cartoon movie clips. Regional brain activity, time-varying and stationary functional connectivity were calculated, and associations with age, sex, and behavioral assessments were examined. Using a model comparison method, we showed that time-varying connectivity was more sensitive to age and sex effects compared with stationary connectivity. The preferred age models were quadratic log age or quadratic age effects, corresponding to inverted-U shaped developmental curves. In addition, females showed higher consistency in regional brain activity and time-varying connectivity than males. However, in terms of behavioral predictions, only stationary connectivity could predict full-scale intelligence quotient. The results suggest that individual differences in time-varying and stationary connectivity may reflect different aspects of behavioral phenotypes.

Keywords: brain connectivity, brain development, model comparison, movie watching, time-varying connectivity.

1. Introduction

Functional integration between spatially remote brain regions is thought to be critical to understanding brain functions. Functional connectivity is characterized by the statistical dependency between observed brain signals (Friston, 1994). This stationary characterization of functional connectivity can be studied during the resting-state (Biswal et al., 1995, 2010), and has furthered our understanding of brain functional organization (Biswal et al., 2010; Margulies et al., 2016; Yeo et al., 2011). On the other hand, functional connectivity is also highly dynamic (Allen et al., 2014). Whole-brain dynamic connectivity patterns constitutes different "states" (Allen et al., 2014), which are reliable (Abrol et al., 2017). Disruptions to dynamic connectivity have been associated with varies mental disorders (Fu et al., 2019).

In recent years, movie watching has emerged as an alternative paradigm between the unconstrained resting-state and well controlled task experiments. Participants' experience when watching video clips is more "natural" than performing some cognitive tasks. In addition, movie watching bears advantages over resting-state in terms of scanning compliance and with potentially lower head motion artifacts (Vanderwal et al., 2019). When watching the same movie clip, different participants tend to show similar patterns of brain activity (Hasson et al., 2004), which could be taken as an indicator of functional significance of the observed brain activity. Time-varying connectivity also shows high constancy across participants (Di et al., 2022; Di and Biswal, 2020), which supports the functional significance of time-varying measures of functional connectivity.

Time-varying and stationary functional connectivity may reflect distinct aspects of brain function. Many studies have found that the stationary connectivity during watching of different movies is very similar (Di et al., 2022; O'Connor et al., 2017; Tian et al., 2021), and may even be highly correlated with other mental states, such as resting-state (O'Connor et al., 2017). On the other hand, time-varying connectivity can depend on the movie content, thus dynamic patterns and region pairs involved have been shown to vary greatly between different movie clips (Di et al., 2022). This seems to suggest that the time-varying connectivity may be more sensitive to reflect moment-to-moment brain function. More generally, during resting-state, time-varying connectivity can capture unique behavioral variability compared with

stationary connectivity (Eichenbaum et al., 2021). A handful studies on disease classifications showed that resting-state time-varying connectivity has better predictive power than stationary connectivity to classify schizophrenia, bipolar disorder (Rashid et al., 2016), and post-traumatic stress disorder (Jin et al., 2017).

To further explore the functional relevance of time-varying and stationary connectivity, we aim to examine individual differences in time-varying and stationary connectivity during movie watching. Age and biological sex are common factors that give rise to individual variations. When watching movie clips, adults showed higher synchronized regional activity compared with children (Cantlon and Li, 2013; Petroni et al., 2018), but children may show distinct patterns of responses compared with adults (Di and Biswal, 2022). A few studies have examined age effects on time-varying and stationary connectivity in the resting-state (Faghiri et al., 2018; Marusak et al., 2017; Rashid et al., 2018). They found linear correlations between some dynamic connectivity measures and age. In the current study, we utilized more complex age models and a model comparison framework to examine age effects. We asked whether time-varying and stationary connectivity differently represent age and sex effects.

Further, we ask whether individual differences in time-varying and stationary connectivity are associated with behavioral outcome measures. In the resting-state, time-varying connectivity performed better than stationary connectivity in predicting behavioral phenotypes (Eichenbaum et al., 2021) and in classification of mental disorders (Jin et al., 2017; Rashid et al., 2016), and post-traumatic stress disorder (Jin et al., 2017). Therefore, it is reasonable to expect that the time-varying connectivity during movie watching may also perform better than stationary connectivity in predicting behavioral outcome measures.

In the current study, we analyzed movie watching fMRI data from a large open-access dataset called the Healthy Brain Network (HBN) (Alexander et al., 2017). A few studies have utilized this dataset to examine model-based brain activations (Richardson, 2019), stationary connectivity (Vanderwal et al., 2021), and event segmentation (Cohen et al., 2022) during the movie watching. Female and male participants age between 5 to 22 years were recruited in this project, with rich behavioral assessments and MRI scanning. From the fMRI data during movie watching, we calculated regional activity, stationary

connectivity, and time-varying connectivity. We used a model comparison framework to examine the age and sex effects on the different brain measures, and adopted a predictive modeling approach to examine the prediction power of these brain measures on behavioral measures. We hypothesize that time-varying connectivity will show stronger evidence of age and sex effects compared with stationary connectivity and regional activity, and time-varying connectivity will also show higher prediction power than stationary connectivity and regional activity in predicting behavioral outcomes.

2. Materials and Methods

2.1. Healthy Brain Network dataset

2.1.1. Dataset and participants

The MRI data were obtained from the Healthy Brain Network project website (http://fcon_1000.projects.nitrc.org/indi/cmi_healthy_brain_network/) (Alexander et al., 2017). We identified 279 participants who have no diagnosis of any psychiatric or neurological disorders and have T1 weighted MRI data available (up to Release 9). We performed stringent quality control on the T1 weighted structural images and fMRI images (see below for details). 159 participants' structural images were found with motion artifacts or lesions. After additionally removing participants with excessive head motion during fMRI scans (maximal framewise displacement smaller than one voxel), 87 participants for 'The Present' dataset and 83 participants for the 'Despicable Me' dataset were included in the current analysis. Among them, 66 participants overlapped. For all the included participants, there were 61 males and 43 females (age range 5.0 to 21.9 years, *Mean = 12.0*; *Standard Deviation = 4.1*).

2.1.2. MRI data

We analyzed fMRI data collected while the participants watched two animated movie clips. The first is a short film 'The Present' (3 minutes and 21 seconds long, Filmakademie Baden-Wuerttemberg, 2014). The second is a 10-minute clip from the animated film 'Despicable Me' (Illumination, 2010). The high-resolution anatomical MRI images were also used for preprocessing purposes.

MRI data were acquired from two MRI centers, Rutgers University Brain Imaging Center (RUBIC), with a 3T Siemens Trio scanner, and Citigroup Biomedical Imaging Center (CBIC), with a 3T Siemens Prisma scanner. The scanning protocols were similar across sites. For fMRI, the key imaging parameters were as follows: TR = 800 ms; TE = 30 ms; flip angle, 31^{o}; voxel size = 2.4 x 2.4 x 2.4 mm^{3}; multi-band acceleration factor = 6. For T1 weighted anatomical MRI, the images were acquired using either the Human Connectome Project (HCP) or the Adolescent Brain Cognitive Development (ABCD) sequences. The sequences are different in terms of voxel sizes, however, the anatomical images were only used for preprocessing of the fMRI images. For more information about the MRI protocols, please refer to the HBN project website and (Alexander et al., 2017).

2.1.3. Behavioral measures

We picked two behavioral measures, full-scale intelligence quotient (FSIQ) from the Wechsler Intelligence Scale for Children – Fifth Edition (Wechsler, 2014) and the Social Communication Questionnaire (SCQ) (Rutter et al., 2003). FSIQ measures general cognitive ability, which is widely used in studies of brain-behavior relationships (Vieira et al., 2022). 64 and 60 participants with the video clip 'The Present' and with the clip 'Despicable Me' had FSIQ scores available, respectively. SCQ is a parent report questionnaire that measures social and communication symptoms related to autism spectrum disorder. In a previous work using the same dataset, it has been reported that the SCQ scores were associated with brain activation during certain time points (events) (Richardson, 2019). 70 and 65 participants with the video clip 'The Present' and the clip 'Despicable Me' had SCQ scores available, respectively.

2.2. MRI data processing

2.2.1. Structural MRI quality control and processing

We visually inspect the MRI images for all the participants. Issues noted included excessive head motion, partial coverage, or brain lesions. We performed visual quality control on the T1 weighted images as well as segmented images. 159 participants' images were found with ghost artifacts, motion artifacts, or lesions. MRI data of 120 participants were included in the current analysis.

Statistical parametric mapping (SPM12, https://www.fil.ion.ucl.ac.uk/spm/) in MATLAB (R2021a, https://www.mathworks.com/) was used for MRI image processing. The T1 weighted image for each participant was first segmented into gray matter, white matter, cerebrospinal fluid, and other tissue types, and roughly aligned into standard Montreal Neurological Institute (MNI) space using linear transformation. Then the DARTEL procedure was used to register the segmented gray matter and white images across all the individuals and generate a sample specific template through several rounds of iterations (Ashburner, 2007). The averaged gray matter template was then linearly normalized to MNI space.

2.2.2. Functional images preprocessing

Functional images were realigned to the first image, coregistered to the anatomical image, and then normalized into MNI space. During the normalization step, the functional images were resampled into 2.4 x 2.4 x 2.4 mm^3 voxel size, and spatially smoothed using an 8 mm Gaussian kernel. Lastly, voxel-wise general linear model (GLM) was used to remove head motion artifacts and low-frequency drifts. The GLM included Friston's 24 head motion parameters (Friston et al., 1996), and 1/128 Hz high pass filter. The residual images from the GLM step were used for further analysis.

Head motion is considered an important factor that affects BOLD fMRI signals. We removed participants who's maximum framewise displacement in any directions or movie clips were larger than 2.4 mm or 2.4^o (proximately the size of a voxel). Next, we examined the association of head motion and the observed age effects. First, we showed that the frame-wise displacement time series were not synchronized across subjects. The first PC explained less than 5% of variance (Figure S1A). Secondly, we used mean frame-wise displacements in translation and rotation as measures of head motion, and examined their age effects. Model comparison showed that for 'The Present' clip, a constant model without age effects was favorable (Figure S1C and S1D). However, for the 'Despicable Me' clip, there was evidence of log age effects (Figure S1E and S1F). The age effect patterns on head motion look very different from the age effects on the brain measures. Nevertheless, we added mean framewise displacement of translation and rotation in the age fitting models.

2.2.4. Independent component analysis

We first utilized independent component analysis (ICA) to reduce the dimensionality of the fMRI data (Di et al., 2022; Di and Biswal, 2022). The ICA was performed using the Group ICA Of fMRI Toolbox(GIFT) (Calhoun et al., 2001) with data from both video clips combined together. Twenty independent components (ICs) were extracted and visually inspected. Eighteen components were considered functional meaningful networks. Based on our previous work (Di et al., 2022; Di and Biswal, 2022). Four networks are specifically of interest due their involvement in movie watching (Di et al., 2022; Di and Biswal, 2022): the dorsal visual network, temporoparietal junction, supramarginal network, and the default mode network (particularly the posterior cingulate cortex) (Figure 1A). The time series for each of the 18 networks were back reconstructed for each participant and video clip, which were used for further analysis.

2.3. Statistical analysis

2.3.1. Regional activity and connectivity measures

Inter-subject correlation has been used to index shared responses during movie watching (Hasson et al., 2004; Nastase et al., 2019). Here we used a principal component analysis (PCA) based method to estimate inter-individual consistency (Di and Biswal, 2022). For each network (IC), the time series from each participant formed a *t* x *n* matrix, where *t* and *n* represent the number of time points and participants, respectively. The matrices were *250* x *87* for the clip 'The Present', and *750* x *83* for the clip 'Despicable Me'. We performed PCA on the matrix, and obtained the variances explained by the first and second PCs. A circular time-shift randomization method was used to determine the null distribution with 10,000 times randomizations (Di and Biswal, 2022; Kauppi et al., 2010). The loadings of the first PC were used as a measure of individual differences.

Between each pair of two networks (ICs), we calculated point-by-point interactions (multiplications) to index time-varying connectivity (Di et al., 2022; Faskowitz et al., 2020). We similarly performed PCA to estimate the inter-individual consistency of the time-varying connectivity. The loadings of the first PC were used as an index of individual differences in time-varying connectivity.

Lastly, we calculated stationary connectivity as the Pearson's correlation of the time series between each pair of the 18 networks (ICs).

2.3.2. Age and sex effects

We adopted a model comparison framework to examine age and sex effects on regional activity, stationary connectivity, and time-varying connectivity. For each region or region pair of a brain measure, we built five models of age effects, with sex as a separate regressor. Additional covariates included a scanner site variable and mean framewise displacement in translation and rotation. The five models are as follows,

$$y = \beta_0 + \beta_1 \cdot sex + \beta_2 \cdot site + \beta_3 \cdot FD_{Trans} + \beta_4 \cdot FD_{Rot} + \varepsilon \quad (1)$$

$$y = \beta_0 + \beta_1 \cdot age + \beta_2 \cdot sex + \beta_3 \cdot site + \beta_4 \cdot FD_{Trans} + \beta_5 \cdot FD_{Rot} + \varepsilon \quad (2)$$

$$y = \beta_0 + \beta_1 \cdot age + \beta_2 \cdot age^2 + \beta_3 \cdot sex + \beta_4 \cdot site + \beta_5 \cdot FD_{Trans} + \beta_6 \cdot FD_{Rot} + \varepsilon \quad (3)$$

$$y = \beta_0 + \beta_1 \cdot \log(age) + \beta_2 \cdot sex + \beta_3 \cdot site + \beta_4 \cdot FD_{Trans} + \beta_5 \cdot FD_{Rot} + \varepsilon \quad (4)$$

$$y = \beta_0 + \beta_1 \cdot \log(age) + \beta_2 \cdot \log(age)^2 + \beta_3 \cdot sex + \beta_4 \cdot site + \beta_5 \cdot FD_{Trans} + \beta_6 \cdot FD_{Rot} + \varepsilon \quad (5)$$

Where y represents a specific measure such as regional activity in a network, stationary connectivity, or time-varying connectivity between two networks. Model 1 represents a baseline condition where there is no age effect. Models 2 and 3 represent linear age effect and quadratic age effect models. Models 4 and 5 represent log age effect and quadratic log age effect models. The log age models consider the fact that brain measures may grow faster and then decrease slower within the studied age range. We additionally built five models the same as models 1 through 5 except that there were no sex effects in each of the models. Therefore, we had 10 models in total (2 x 5).

To compare different age models and sex effects, we used a model comparison procedure. The 10 models were fitted with the ordinary least square method, and the Akaike information criterion (AIC) was calculated. We then calculated Akaike weights (Wagenmakers and Farrell, 2004) for each model. Akaike weights quantify the model evidence of a specific model relative to the best model among all the 10 models, with the sum of all the models as 1. We first asked what age model best to describe the

developmental effects. The Akaike weights of the same age model with and without the sex term were added as the model evidence of a particular age effect, regardless of the sex effects (Portet, 2020). Similarly, for the sex effect, we added the Akaike weights for all five age models with the sex term. The sums of model weights depend on the number of alternative models. We adopt a threshold of 0.6 for the age model comparison (5 models) and 0.8 for the sex effect comparison (2 models).

2.3.3. Behavioral prediction analysis

We applied ridge regression to study brain-behavioral associations. The predicted variable was either FSIQ scores or SCQ scores, which was an *n* by *1* vector. *N* were different for FSIQ and SCQ scores and for the two movie clips due to data availability. The predicting variables were either regional activity, stationary connectivity, or time-varying connectivity. We applied a leave-one-out cross-validation to evaluate the prediction value for each brain measure. Specifically, we held out one participant's data, and used the remaining *n – 1* data to obtain a prediction model. We used a linear model for the prediction.

$$y = \beta_0 + X \cdot \beta + \varepsilon$$

where *y* is a *n – 1* vector of either FSIQ of SCQ scores, *X* is a *n – 1* by *m* matrix of regional activity, stationary connectivity, or time-varying connectivity matrices. For the regional activity, *m* equals to 18 of the networks. For the matrices, the number of column equals *153* (*18 x 17 / 2*), which is larger than the number of rows. We used a dimension reduction procedure to keep 18 features to match with the number of regional activity. To do so, all the features were correlated with the predicted variable, and the first 18 features with the highest absolute correlations were kept. Therefore, *X* is always a *n – 1* by *18* matrix. The model was fitted with a ridge regularization. The regularization parameter λ was determined using a nested cross-validation procedure for each training set. Using the optimal λ, the model was trained using the *n – 1* training data. The model was applied to the held-out participant to calculate the predicted value. The procedure was performed *n* times for the *n* participants, resulting in *n* predicted values. We calculated the correlation between the predicted value and the actual values across all n participants to obtain an estimate of prediction accuracy.

The optimal λ was determined for each leave-one-out sample using an inner leave-one-out loop. Within the $n - 1$ outer-loop training set, we built linear models with $n - 2$ individuals with 21 λ values (from 2^{-10} to 2^{0} in logarithmical space). The prediction accuracies across all the inner loop samples were calculated for all the λ values. The λ with the highest correlation was parsed to the outer loop as the optimal λ for model training and prediction. The prediction procedure is outlined in Supplementary Figure S1.

To evaluate the prediction accuracies, we used the correlation coefficient between the predicted and observed values. There are in total 12 predictions (2 movies x 3 brain measures x 2 behavioral measures). We used false discovery rate correction to account for multiple comparisons ($q < 0.05$).

3. Results

3.1. Regional activity

We first focused on the inter-individual consistency and differences in regional activity when watching the two video clips. We performed PCA on the time point by participant matrices of regional activity in each of the 18 included networks (ICs). The first PCs in all the 18 networks explained a statistically significant amount of variance for both videos. However, none of the second PCs explained significant variance. Therefore, we focused on the first PCs in the following analysis. Figure 1B shows the percentage variance explained by the first PC in the 18 networks for the two movie clips. In addition to lower-level sensory networks such as the visual and auditory networks, a few higher-level networks also showed high inter-individual consistency, including the dorsal visual network (IC3), temporoparietal junction network (IC4), supramarginal network (IC7), and default mode network (IC16). There are also noticeable differences between the two video clips. In particular, a network covering the posterior insula, secondary somatosensory regions and cingulate (IC9) showed more than 2 fold in variance explained by the first PC in 'The Present' (23.0%) than 'Despicable Me' (10.0%). We submitted the map to Neurosynth for cognitive decoding (Yarkoni et al., 2011). After removing terms related to brain labels, the top five terms were pain, painful, tactile, stimulation, and touch.

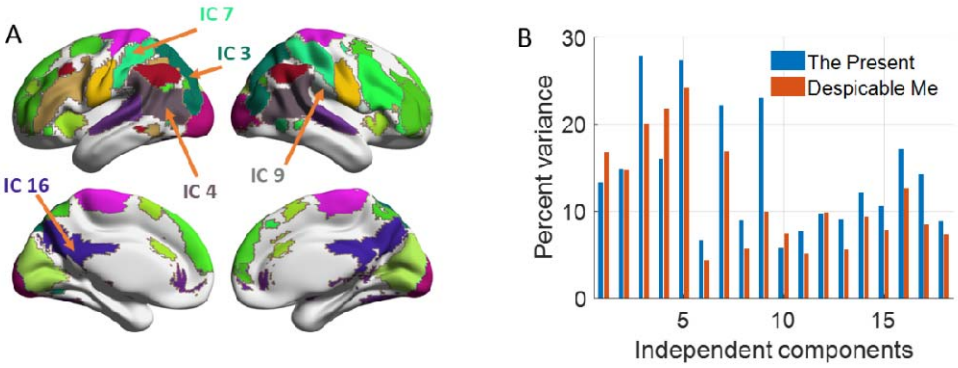

Figure 1 A, Maps of eighteen independent components that were included in the current analysis. The maps were thresholded at z > 3 after z transformations of the original IC maps, and were shown in a winner-take-all manner when overlapping. The arrows indicate the networks of interest for movie watching, IC3, dorsal visual; IC4, temporoparietal junction; IC7 supramarginal; IC9, secondary somatosensory; and IC16, posterior cingulate. BrainNet Viewer was used for visualization (Xia et al., 2013). B, inter-individual consistency of regional activity (percent variance explained by the first principal component) for the two video clips.

We then applied a model comparison procedure to examine the age and sex effects. Figure 2A and 2B shows the model evidence among the five age models for the 18 network ICs and the two video clips. For the networks with a strong preference of a model, the preferred model was usually the quadratic log age or quadratic age model. We identified the network ICs where a specific age model had model evidence higher than 0.6, and plotted the fitted effects in Figure 2D and 2F. All the age effects showed an inverted-U shape, with peak loadings around 10 years of age. The quadratic log age models indicated a faster increase in the younger age and slower decrease in older age. Figure 2E and 2G further show individual loadings as well as the fitted curves for the two curves on the top of Figure 2D and 2F. Figure 2E corresponds to the supramarginal network (IC7) in the video clips of 'The Present', and Figure 2G corresponds to the bilateral parietal junction network (IC4) in the 'Despicable Me' clip.

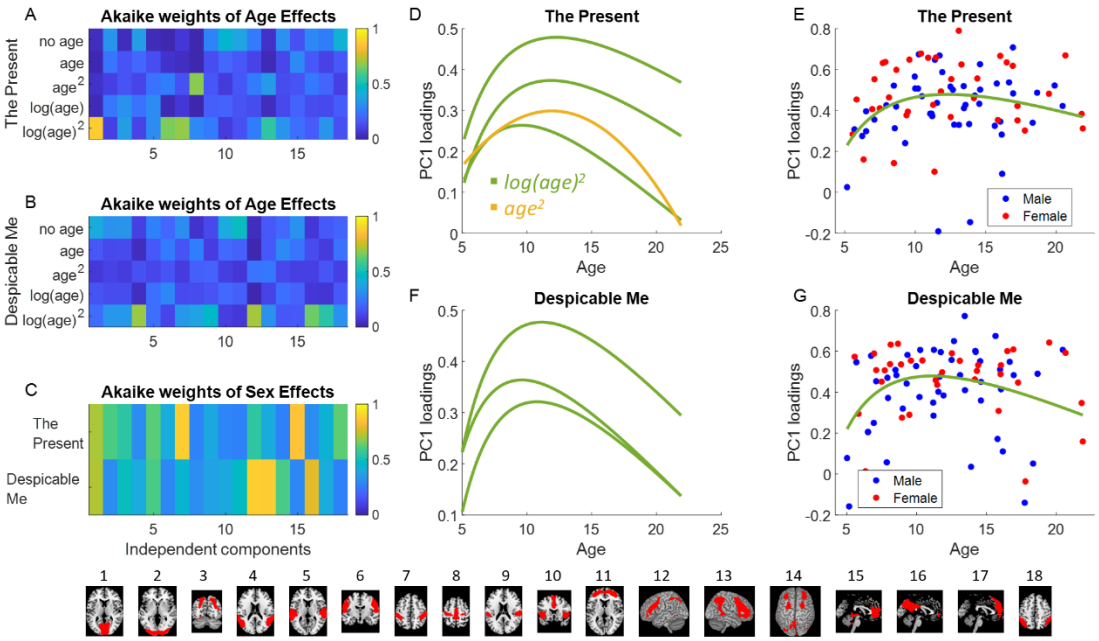

Figure 2 Model comparison results for different age models for regional activity in the 18 network independent components (ICs) for the video clips The Present (A) and Despicable Me (B). C shows the model evidence of the sex effects. D and F show fitted effects of the ICs who had Akaike weights of one model over 0.6. E and G show the PC1 loadings of two representative ICs as functions of age, which correspond to the top curves in D and F, respectively.

Four networks showed strong evidence of a sex effect (> 0.8) on regional activity for the two video clips differently (Figure 2C). For 'The Present', the supramarginal network (IC7) (model probability = *88.36%*) and medial frontal network (IC15) (model probability = *85.76%*) showed evidence of sex effects. While for the video clip of 'Despicable Me', the left (IC12) and right (IC13) fronto-parietal networks showed evidence of sex effects (model probability = *88.80%* and *87.50%*, respectively). For all the effects, the females showed higher consistency than the males.

3.2. Stationary connectivity

The group averaged stationary connectivity matrices for the two video clips are shown in Figure 3A and 3E. The two matrices were similar, which is in line with our previous work (Di et al., 2022). Higher stationary connectivity was observed mainly between networks with similar functions, e.g., among visual networks and among fronto-parietal networks.

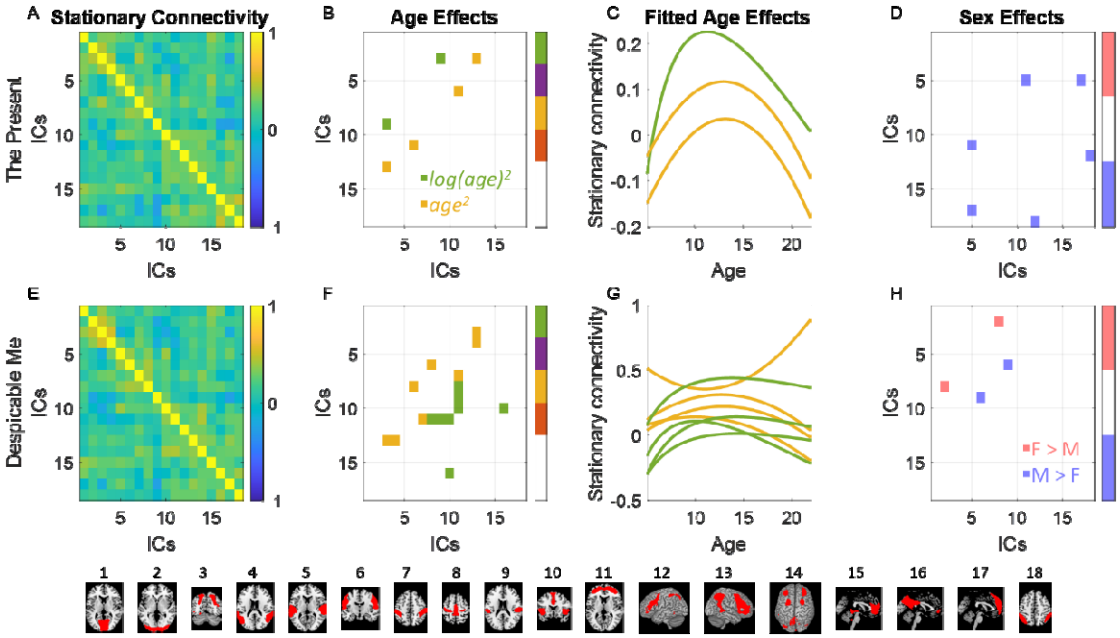

Figure 3 A and E, group averaged stationary connectivity among 18 independent component (IC) networks for the two video clips. B and F, connectivity with winning age models with model evidence greater than 0.6. C and G, fitted curves with corresponding color representing the specific age models. D and H, connectivity with evidence of sex effects greater than 0.8. The bottom row shows the representative maps of the 18 networks.

The model comparison results for the age and sex effects on the stationery are shown in Supplementary Figure S3. The connections that showed preferences of an age model with greater than 0.6 model evidence are shown in Figure 3B and 3F. The preferred age models were either quadratic log age or quadratic age models. All but one age effects showed an inverted-U shapes (Figure 3C and 3G). Three connections showed a preference of an age model for the clip of 'The Present', and eight connections showed a preference of an age model for the 'Despicable Me' video. One stationary connectivity during

'The Present' involved two networks of interest, i.e., the dorsal visual network (IC3) and secondary somatosensory network (IC9). And the patterns of age effects appeared to be quite different for the two video clips. In addition, three connections for the clip of 'The Present' and two connections for the 'Despicable Me' clip showed sex effects, but they were not among the networks of interests related to movie watching.

3.3. Time-varying connectivity

Figure 4A and 4E show the consistency of time-varying connectivity for the two movie clips. In general, the clips of 'The Present' showed higher consistency of time-varying connectivity. Interestingly, the time-varying connectivity among many networks of interest, i.e., the dorsal visual network (IC3), supramarginal network (IC7), and secondary somatosensory network (IC9) showed high consistency. Moreover, the medial prefrontal network (IC17), which is part of the default mode network, also showed consistent time-varying connectivity with the other regions of interest.

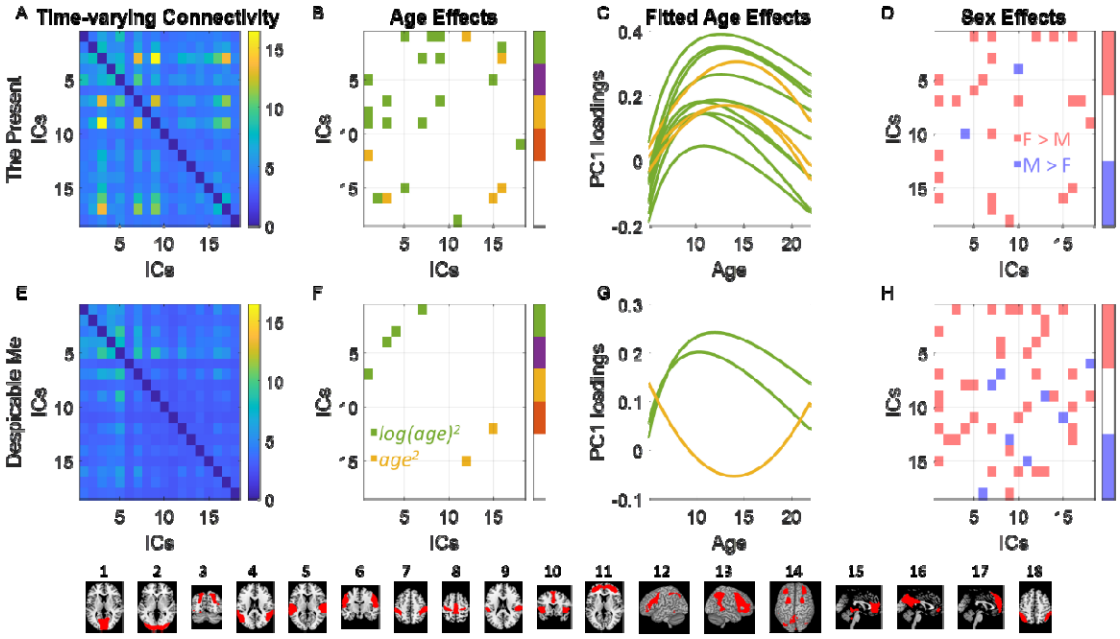

Figure 4 A and E, the inter-individual consistency of time-varying connectivity (percent variance explained by the first principal component) among 18 networks (independent components, ICs) for the two video clips. B and F, connectivity with winning age models with model evidence greater than 0.6. C

and G, fitted curves with corresponding color representing the specific age models. D and H, connectivity with evidence of sex effects greater than 0.8. The bottom row shows the representative maps of the 18 networks.

The age effects on time-varying connectivity also preferred quadratic log age or quadratic age effects (Supplementary Figure S3 and Figure 4B and 4F). Fourteen connections showed strong preferences to an age model for the video 'The Present'. Interestingly, time-varying connectivity among the dorsal visual (IC3), supramarginal (IC7), and secondary somatosensory (IC9) networks strongly preferred the quadratic log age effects. In contrast, only three connections showed strong preferences to an age model for the video 'Despicable Me'.

Many connections also showed strong evidence of sex effects, mainly with higher consistency in females than males (Figure 4D and 4H). This included time-varying connectivity between the dorsal visual (IC3) and the supramarginal networks (IC7).

3.4. Behavioral relevance

Lastly, we used machine learning regression to examine the behavioral relevance of regional activity, stationary connectivity, and time-varying connectivity. Two behavioral measures were studied: FSIQ and SCQ scores. With leave-one-out cross-validation, we estimated the prediction accuracy of the three types of brain measures on FSIQ and SCQ scores. Only stationary connectivity showed statistically significant prediction accuracies (Figure 5). Using stationary connectivity from both video clips, we could predict FSIQ scores with accuracies of around 0.35. Individual differences of regional activity and time-varying connectivity could not predict FSIQ scores (Supplementary Figure S5). In addition, none of the brain measures could predict SCQ scores (Supplementary Figure S6).

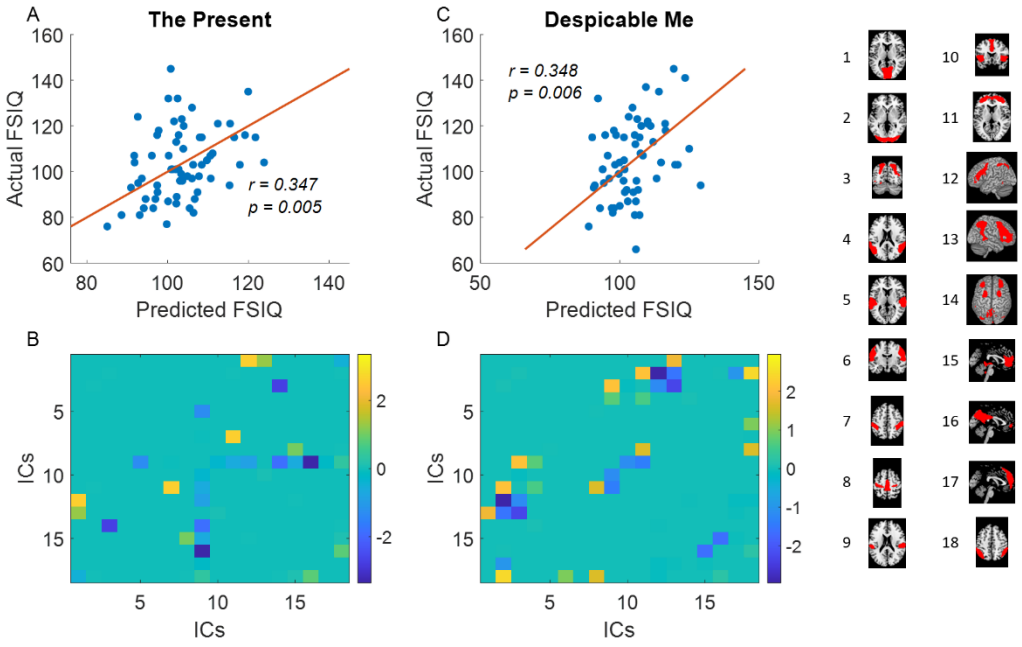

Figure 5 Results of full-scale intelligence quotient (FSIQ) predictions using stationary connectivity for the two video clips. Top row, each dot represents a predicted value using leave-one-out cross validation and its corresponding actual value. The red line indicates $y = x$. Bottom row, averaged weights of the prediction model across all the LOO models. The maps of the corresponding independent components (ICs) are shown on the right.

4. Discussion

In the current study, we examined individual differences in stationery and time-varying connectivity, as well as regional activity, during movie watching in a sample of children to young adults. Consistent with our hypothesis, time-varying connectivity was more sensitive to age and sex effects compared with stationary connectivity and regional activity. In contrast to our hypothesis, however, only stationary connectivity could predict FSIQ scores.

The two animated video clips evoked consistent brain activations across individuals in higher order brain regions, including the dorsal visual, temporoparietal junction, supramarginal, and the default

mode networks, which have shown similar consistent responses with different movie clips and samples (Di et al., 2022; Di and Biswal, 2022). Many of these regions, e.g., the temporoparietal junction, supramarginal, and default mode networks are involve in processing of higher order social information, as might be expected during watching of the movie clips. More interestingly, a unique independent component covering the secondary somatosensory cortex, posterior insula, and cingulate cortex showed much higher consistency in the clip of 'The Present' compared with the clip of 'Despicable Me'. These regions are related to higher somatosensory and pain process, and may be involved in empathy for pain (Allen et al., 2017; Lamm et al., 2007). Because 'The Present' involves a scene of an amputated limb, it is reasonable that these regions are involved. Our discussions will focus on these networks.

For all the connectivity and activity measures, the optimal age models were quadratic log-age or age effects, mostly exhibiting an inverted-U shape. Time-varying and stationary connectivity showed age effects in different connections, with time-varying connectivity showing age effects between regions related to movie watching. The inverted-U shape indicates that the brain measures increase during early childhood and later decrease toward adulthood. This provides a more complete picture of synchronized responses compared with previous studies with only two groups of adults and children (Cantlon and Li, 2013; Petroni et al., 2018). The reduced synchrony in adults compared with teen age children may indicate that neural processing is more efficient in adults therefore requiring less activation. Alternatively, the adult participants may have more idiosyncratic responses to the video clips, or the cartoon nature may make the adult participants less engaged in watching them. Nevertheless, a practical implication is that when controlling for age effects, a simple linear model may not be sufficient.

We observed widespread sex effects for time-varying connectivity, with females having higher consistency than males. This may due to the fact that many cognitive process involve higher levels of brain activation in females than males, e.g., empathy for pain (Christov-Moore and Iacoboni, 2019; Groen et al., 2013) and language processing (Burman et al., 2008). But due to the complexity of the movie stimuli, it is difficult to pinpoint a specific cognitive process that solely explains the observed sex differences. Moreover, sex differences may interact with other factors such as age (Etchell et al., 2018).

We did not explore the interaction effects in the current study due to the limited sample size, but this effect needs to be studied in future works with larger samples.

In contrast to our hypothesis, the behavioral prediction analyses showed that only stationary connectivity, but not time-varying connectivity or regional activity, could predict FSIQ scores. Stationary connectivity could reliably predict FSIQ from both the video clips. The contents of the movie clips involve social interactions, which may not be related to general intelligence abilities. Indeed, brain regions that are generally associated with FSIQ are higher-order association regions, such as the lateral prefrontal cortex (Cole et al., 2012; Geake and Hansen, 2005). The prediction features in the current analysis (Figure 5C and 5D) supported this point. Because stationary connectivity remains stable across different conditions, it may reflect general characteristics of cognitive functions, such as FSIQ (Finn and Bandettini, 2021). On the other hand, time-varying connectivity may be sensitive to certain movie contents, therefore not reflecting general cognitive ability. In terms of the SCQ scores, none of the brain measures could predict individual differences in SCQ scores. The SCQ score was chosen because it reflects deficits in social functions related to autism. A study has reported an association between brain activity and SCQ scores at certain time points using the same HBN dataset (Richardson, 2019). With a whole-brain predictive modeling approach with cross-validation, we could not find reliable associations between brain measures and SCQ scores. The association may exist, but be restricted to brain activity during certain events. Alternatively, in this normative sample there may not be a large range of SCQ scores. Therefore, the association between brain measures and SCQ scores in a healthy sample may be weak.

The current study analyzed two animated video clips. Many aspects of individual differences appeared to be different between the two clips. For example, the preferred age models and sex effects for both the stationery and time-varying connectivity turned out to be very different between the two clips. This suggests that many of the individual differences depend on the specific movie stimuli. On one hand, this may be desirable, because different movie stimuli may be used to probe different brain functions. On

the other hand, this means that one should be careful when interpreting results of movie watching studies, as they might be highly sensitive to the stimuli presented.

5. Conclusion

In the current study, we examined age and sex effects, and behavioral correlates of time-varying and stationary connectivity during movie watching. We found that time-varying connectivity is more sensitive to the age and sex effects. However, only stationary connectivity could predict individuals' FSIQ scores. These results provide a more detailed portrait of individual differences in time-varying and stationary connectivity in the human brain.

Acknowledgement:

This study was supported by (US) National Institute of Mental Health grants to X.D. (R15MH125332) and B.B.B. (R01MH131335). The authors would like to thank Donna Chen for her comments on earlier versions of this manuscript.

Reference:

Abrol, A., Damaraju, E., Miller, R.L., Stephen, J.M., Claus, E.D., Mayer, A.R., Calhoun, V.D., 2017. Replicability of time-varying connectivity patterns in large resting state fMRI samples. NeuroImage 163, 160–176. https://doi.org/10.1016/j.neuroimage.2017.09.020

Alexander, L.M., Escalera, J., Ai, L., Andreotti, C., Febre, K., Mangone, A., Vega-Potler, N., Langer, N., Alexander, A., Kovacs, M., Litke, S., O'Hagan, B., Andersen, J., Bronstein, B., Bui, A., Bushey, M., Butler, H., Castagna, V., Camacho, N., Chan, E., Citera, D., Clucas, J., Cohen, S., Dufek, S., Eaves, M., Fradera, B., Gardner, J., Grant-Villegas, N., Green, G., Gregory, C., Hart, E., Harris, S., Horton, M., Kahn, D., Kabotyanski, K., Karmel, B., Kelly, S.P., Kleinman, K., Koo, B., Kramer, E., Lennon, E., Lord, C., Mantello, G., Margolis, A., Merikangas, K.R., Milham, J., Minniti, G., Neuhaus, R., Levine, A., Osman, Y., Parra, L.C., Pugh, K.R., Racanello, A., Restrepo, A., Saltzman, T., Septimus, B., Tobe, R., Waltz, R., Williams, A., Yeo, A., Castellanos, F.X., Klein, A., Paus, T., Leventhal, B.L., Craddock, R.C., Koplewicz, H.S., Milham, M.P., 2017. An open resource for transdiagnostic research in pediatric mental health and learning disorders. Scientific Data 4, 1–26. https://doi.org/10.1038/sdata.2017.181

Allen, E.A., Damaraju, E., Plis, S.M., Erhardt, E.B., Eichele, T., Calhoun, V.D., 2014. Tracking whole-brain connectivity dynamics in the resting state. Cerebral cortex (New York, N.Y.□: 1991) 24, 663–76. https://doi.org/10.1093/cercor/bhs352

Allen, M., Frank, D., Glen, J.C., Fardo, F., Callaghan, M.F., Rees, G., 2017. Insula and somatosensory cortical myelination and iron markers underlie individual differences in empathy. Sci Rep 7, 43316. https://doi.org/10.1038/srep43316

Ashburner, J., 2007. A fast diffeomorphic image registration algorithm. NeuroImage 38, 95–113. https://doi.org/10.1016/j.neuroimage.2007.07.007

Biswal, B., Yetkin, F.Z., Haughton, V.M., Hyde, J.S., 1995. Functional connectivity in the motor cortex of resting human brain using echo-planar MRI. Magnetic resonance in medicine□: official journal of the Society of Magnetic Resonance in Medicine / Society of Magnetic Resonance in Medicine 34, 537–41. https://doi.org/10.1002/mrm.1910340409

Biswal, B.B., Mennes, M., Zuo, X.-N., Gohel, S., Kelly, C., Smith, S.M., Beckmann, C.F., Adelstein, J.S., Buckner, R.L., Colcombe, S., Dogonowski, A.-M., Ernst, M., Fair, D., Hampson, M., Hoptman, M.J., Hyde, J.S., Kiviniemi, V.J., Kötter, R., Li, S.-J., Lin, C.-P., Lowe, M.J., Mackay, C., Madden, D.J., Madsen, K.H., Margulies, D.S., Mayberg, H.S., McMahon, K., Monk, C.S., Mostofsky, S.H., Nagel, B.J., Pekar, J.J., Peltier, S.J., Petersen, S.E., Riedl, V., Rombouts, S.A.R.B., Rypma, B., Schlaggar, B.L., Schmidt, S., Seidler, R.D., Siegle, G.J., Sorg, C., Teng, G.-J., Veijola, J., Villringer, A., Walter, M., Wang, L., Weng, X.-C., Whitfield-Gabrieli, S., Williamson, P., Windischberger, C., Zang, Y.-F., Zhang, H.-Y., Castellanos, F.X., Milham, M.P., 2010. Toward discovery science of human brain function. Proceedings of the National Academy of Sciences of the United States of America 107, 4734–9. https://doi.org/10.1073/pnas.0911855107

Burman, D.D., Bitan, T., Booth, J.R., 2008. Sex differences in neural processing of language among children. Neuropsychologia 46, 1349–1362. https://doi.org/10.1016/j.neuropsychologia.2007.12.021

Calhoun, V.D., Adali, T., Pearlson, G.D., Pekar, J.J., 2001. A method for making group inferences from functional MRI data using independent component analysis. Human brain mapping 14, 140–51.

Cantlon, J.F., Li, R., 2013. Neural Activity during Natural Viewing of Sesame Street Statistically Predicts Test Scores in Early Childhood. PLOS Biology 11, e1001462. https://doi.org/10.1371/journal.pbio.1001462

Christov-Moore, L., Iacoboni, M., 2019. Sex differences in somatomotor representations of others' pain: a permutation-based analysis. Brain Struct Funct 224, 937–947. https://doi.org/10.1007/s00429-018-1814-y

Cohen, S.S., Tottenham, N., Baldassano, C., 2022. Developmental changes in story-evoked responses in the neocortex and hippocampus. eLife 11, e69430. https://doi.org/10.7554/eLife.69430

Cole, M.W., Yarkoni, T., Repovš, G., Anticevic, A., Braver, T.S., 2012. Global Connectivity of Prefrontal Cortex Predicts Cognitive Control and Intelligence. J. Neurosci. 32, 8988–8999. https://doi.org/10.1523/JNEUROSCI.0536-12.2012

Di, X., Biswal, B.B., 2022. Principal component analysis reveals multiple consistent responses to naturalistic stimuli in children and adults. Human Brain Mapping 43, 3332–3345. https://doi.org/10.1002/hbm.25568

Di, X., Biswal, B.B., 2020. Intersubject consistent dynamic connectivity during natural vision revealed by functional MRI. NeuroImage 116698. https://doi.org/10.1016/j.neuroimage.2020.116698

Di, X., Zhang, Z., Xu, T., Biswal, B.B., 2022. Dynamic and stationary brain connectivity during movie watching as revealed by functional MRI. Brain Struct Funct. https://doi.org/10.1007/s00429-022-02522-w

Eichenbaum, A., Pappas, I., Lurie, D., Cohen, J.R., D'Esposito, M., 2021. Differential contributions of static and time-varying functional connectivity to human behavior. Network Neuroscience 5, 145–165. https://doi.org/10.1162/netn_a_00172

Etchell, A., Adhikari, A., Weinberg, L.S., Choo, A.L., Garnett, E.O., Chow, H.M., Chang, S.-E., 2018. A systematic literature review of sex differences in childhood language and brain development. Neuropsychologia 114, 19–31. https://doi.org/10.1016/j.neuropsychologia.2018.04.011

Faghiri, A., Stephen, J.M., Wang, Y.-P., Wilson, T.W., Calhoun, V.D., 2018. Changing brain connectivity dynamics: From early childhood to adulthood. Human Brain Mapping 39, 1108–1117. https://doi.org/10.1002/hbm.23896

Faskowitz, J., Esfahlani, F.Z., Jo, Y., Sporns, O., Betzel, R.F., 2020. Edge-centric functional network representations of human cerebral cortex reveal overlapping system-level architecture. Nat Neurosci 23, 1644–1654. https://doi.org/10.1038/s41593-020-00719-y

Finn, E.S., Bandettini, P.A., 2021. Movie-watching outperforms rest for functional connectivity-based prediction of behavior. NeuroImage 235, 117963. https://doi.org/10.1016/j.neuroimage.2021.117963

Friston, K.J., 1994. Functional and effective connectivity in neuroimaging: A synthesis. Human Brain Mapping 2, 56–78. https://doi.org/10.1002/hbm.460020107

Friston, K.J., Williams, S., Howard, R., Frackowiak, R.S., Turner, R., 1996. Movement-related effects in fMRI time-series. Magnetic resonance in medicine : official journal of the Society of Magnetic Resonance in Medicine / Society of Magnetic Resonance in Medicine 35, 346–55. https://doi.org/DOI 10.1002/mrm.1910350312

Fu, Z., Tu, Y., Di, X., Du, Y., Sui, J., Biswal, B.B., Zhang, Z., de Lacy, N., Calhoun, V.D., 2019. Transient increased thalamic-sensory connectivity and decreased whole-brain dynamism in autism. NeuroImage 190, 191–204. https://doi.org/10.1016/j.neuroimage.2018.06.003

Geake, J.G., Hansen, P.C., 2005. Neural correlates of intelligence as revealed by fMRI of fluid analogies. NeuroImage 26, 555–564. https://doi.org/10.1016/j.neuroimage.2005.01.035

Groen, Y., Wijers, A.A., Tucha, O., Althaus, M., 2013. Are there sex differences in ERPs related to processing empathy-evoking pictures? Neuropsychologia 51, 142–155. https://doi.org/10.1016/j.neuropsychologia.2012.11.012

Hasson, U., Nir, Y., Levy, I., Fuhrmann, G., Malach, R., 2004. Intersubject synchronization of cortical activity during natural vision. Science (New York, N.Y.) 303, 1634–40. https://doi.org/10.1126/science.1089506

Jin, C., Jia, H., Lanka, P., Rangaprakash, D., Li, L., Liu, T., Hu, X., Deshpande, G., 2017. Dynamic brain connectivity is a better predictor of PTSD than static connectivity. Human Brain Mapping 38, 4479–4496. https://doi.org/10.1002/hbm.23676

Kauppi, J.-P., Jääskeläinen, I.P., Sams, M., Tohka, J., 2010. Inter-subject correlation of brain hemodynamic responses during watching a movie: localization in space and frequency. Front. Neuroinform. 4. https://doi.org/10.3389/fninf.2010.00005

Lamm, C., Nusbaum, H.C., Meltzoff, A.N., Decety, J., 2007. What Are You Feeling? Using Functional Magnetic Resonance Imaging to Assess the Modulation of Sensory and Affective Responses during Empathy for Pain. PLOS ONE 2, e1292. https://doi.org/10.1371/journal.pone.0001292

Margulies, D.S., Ghosh, S.S., Goulas, A., Falkiewicz, M., Huntenburg, J.M., Langs, G., Bezgin, G., Eickhoff, S.B., Castellanos, F.X., Petrides, M., Jefferies, E., Smallwood, J., 2016. Situating the default-mode network along a principal gradient of macroscale cortical organization. PNAS 113, 12574–12579. https://doi.org/10.1073/pnas.1608282113

Marusak, H.A., Calhoun, V.D., Brown, S., Crespo, L.M., Sala-Hamrick, K., Gotlib, I.H., Thomason, M.E., 2017. Dynamic functional connectivity of neurocognitive networks in children. Human Brain Mapping 38, 97–108. https://doi.org/10.1002/hbm.23346

Nastase, S.A., Gazzola, V., Hasson, U., Keysers, C., 2019. Measuring shared responses across subjects using intersubject correlation. Soc Cogn Affect Neurosci 14, 667–685. https://doi.org/10.1093/scan/nsz037

O'Connor, D., Potler, N.V., Kovacs, M., Xu, T., Ai, L., Pellman, J., Vanderwal, T., Parra, L.C., Cohen, S., Ghosh, S., Escalera, J., Grant-Villegas, N., Osman, Y., Bui, A., Craddock, R.C., Milham, M.P., 2017. The Healthy Brain Network Serial Scanning Initiative: a resource for evaluating inter-

566 individual differences and their reliabilities across scan conditions and sessions. Gigascience 6,
567 1–14. https://doi.org/10.1093/gigascience/giw011
568 Petroni, A., Cohen, S.S., Ai, L., Langer, N., Henin, S., Vanderwal, T., Milham, M.P., Parra, L.C., 2018.
569 The Variability of Neural Responses to Naturalistic Videos Change with Age and Sex. eNeuro 5.
570 https://doi.org/10.1523/ENEURO.0244-17.2017
571 Portet, S., 2020. A primer on model selection using the Akaike Information Criterion. Infectious Disease
572 Modelling 5, 111–128. https://doi.org/10.1016/j.idm.2019.12.010
573 Rashid, B., Arbabshirani, M.R., Damaraju, E., Cetin, M.S., Miller, R., Pearlson, G.D., Calhoun, V.D.,
574 2016. Classification of schizophrenia and bipolar patients using static and dynamic resting-state
575 fMRI brain connectivity. NeuroImage 134, 645–657.
576 https://doi.org/10.1016/j.neuroimage.2016.04.051
577 Rashid, B., Blanken, L.M.E., Muetzel, R.L., Miller, R., Damaraju, E., Arbabshirani, M.R., Erhardt, E.B.,
578 Verhulst, F.C., van der Lugt, A., Jaddoe, V.W.V., Tiemeier, H., White, T., Calhoun, V., 2018.
579 Connectivity dynamics in typical development and its relationship to autistic traits and autism
580 spectrum disorder. Human Brain Mapping 39, 3127–3142. https://doi.org/10.1002/hbm.24064
581 Richardson, H., 2019. Development of brain networks for social functions: Confirmatory analyses in a
582 large open source dataset. Developmental Cognitive Neuroscience 37, 100598.
583 https://doi.org/10.1016/j.dcn.2018.11.002
584 Rutter, M., Bailey, A., Lord, C., 2003. The social communication questionnaire.
585 Tian, L., Ye, M., Chen, C., Cao, X., Shen, T., 2021. Consistency of functional connectivity across
586 different movies. NeuroImage 233, 117926. https://doi.org/10.1016/j.neuroimage.2021.117926
587 Vanderwal, T., Eilbott, J., Castellanos, F.X., 2019. Movies in the magnet: Naturalistic paradigms in
588 developmental functional neuroimaging. Developmental Cognitive Neuroscience 36, 100600.
589 https://doi.org/10.1016/j.dcn.2018.10.004
590 Vanderwal, T., Eilbott, J., Kelly, C., Frew, S.R., Woodward, T.S., Milham, M.P., Castellanos, F.X., 2021.
591 Stability and similarity of the pediatric connectome as developmental measures. NeuroImage 226,
592 117537. https://doi.org/10.1016/j.neuroimage.2020.117537
593 Vieira, B.H., Pamplona, G.S.P., Fachinello, K., Silva, A.K., Foss, M.P., Salmon, C.E.G., 2022. On the
594 prediction of human intelligence from neuroimaging: A systematic review of methods and
595 reporting. Intelligence 93, 101654. https://doi.org/10.1016/j.intell.2022.101654
596 Wagenmakers, E.-J., Farrell, S., 2004. AIC model selection using Akaike weights. Psychonomic Bulletin
597 & Review 11, 192–196. https://doi.org/10.3758/BF03206482
598 Wechsler, D., 2014. The Wechsler intelligence scale for children—fifth edition.
599 Xia, M., Wang, J., He, Y., 2013. BrainNet Viewer: a network visualization tool for human brain
600 connectomics. PloS one 8, e68910. https://doi.org/10.1371/journal.pone.0068910
601 Yarkoni, T., Poldrack, R.A., Nichols, T.E., Van Essen, D.C., Wager, T.D., 2011. Large-scale automated
602 synthesis of human functional neuroimaging data. Nature methods 8, 665–70.
603 https://doi.org/10.1038/nmeth.1635
604 Yeo, B.T.T., Krienen, F.M., Sepulcre, J., Sabuncu, M.R., Lashkari, D., Hollinshead, M., Roffman, J.L.,
605 Smoller, J.W., Zöllei, L., Polimeni, J.R., Fischl, B., Liu, H., Buckner, R.L., 2011. The
606 organization of the human cerebral cortex estimated by intrinsic functional connectivity. Journal
607 of neurophysiology 106, 1125–65. https://doi.org/10.1152/jn.00338.2011
608

609

610